



Removal of Methylene Blue Dye from Aqueous Solution Using Trichlorovinylsilane Chitosan-g-polyacrylamide Hydrogel

Anthony U. Awode^{1,2*}, Sunday E. Elaigwu^{3*} , Akeem A. Oladipo¹, Osman Yilmaz¹, Mustafa Gazi^{1*}

¹ Polymeric Materials Research Laboratory, Chemistry Department, Faculty of Arts and Science, Eastern Mediterranean University, TR North Cyprus, Famagusta via Mersin 10, Turkey

² Department of Chemistry, Faculty of Natural Sciences, University of Jos, Plateau State, Nigeria

³ Department of Chemistry, Faculty of Physical Sciences, University of Ilorin, Kwara State, Nigeria.

Abstract: A new hydrogel based on vinylsilane-chitosan and acrylamide was synthesized as VSi-CTS-g-PAAM and was used to remove methylene blue (MB) from aqueous solution using batch adsorption technique. The VSi-CTS-PAAM hydrogel interacted with methylene blue (MB) dye solution at different mass-liquid ratios, pH, and temperature. The amount of MB dye removal was estimated using a UV-Vis spectrophotometer at an optical density of $\lambda_{\max} = 665$ nm. The MB dye removal was most effective at pH 12, with about 98 % removal at 50 °C. The study's findings also indicated that the equilibrium data exhibited the highest degree of conformity with the Langmuir isotherm model. Additionally, the adsorption process adhered to the pseudo-second-order kinetics and was characterized as endothermic. Therefore, our study suggests that the utilization of prepared materials may have potential advantages in treating wastewater containing dyes.

Keywords: Acrylamide, Adsorption, Chitosan, Hydrogel, Vinylsilane.

Submitted: May 4, 2023. **Accepted:** August 21, 2023.

Cite this: Awode AU, Elaigwu SE, Oladipo AA, Yilmaz O, Gazi M. Removal of Methylene Blue Dye from Aqueous Solution Using Trichlorovinylsilane Chitosan-g-polyacrylamide Hydrogel. JOTCSA. 2023;10(4):1009-18.

DOI: <https://doi.org/10.18596/jotcsa.1292604>

***Corresponding author's E-mail:** awodea@unijos.edu.ng; elaigwu.se@unilorin.edu.ng

1. INTRODUCTION

Over 280,000 tonnes per year of various dyes are estimated to be discharged into water bodies globally (1). A good percentage of these dyes are not effectively treated before their release into water bodies and thus pose a substantial environmental challenge to the biodiversity and usability of these water bodies (2). The need to rid water bodies of these dyes from textile effluent is of utmost necessity, as water is becoming a scarce commodity.

Various methods have been developed to treat wastewater; these include adsorption, photocatalytic degradation, biological treatment, chemical oxidation, and precipitation (3). These methods are effective but time-consuming and usually involve high-energy demand, leading to higher costs. An extensive review of the advantages and disad-

vantages of these methods has been published (4,5). Adsorption technology, a hybrid of physical and chemical treatment methods, has gained prominence due to its low operation cost and effectiveness (6-8).

Diverse techniques utilizing low-cost adsorbents have been successfully advanced for dye removal (9,10). In recent years, hydrogel-based materials, which are polymeric materials with three-dimensional networks retaining a large quantity of water within their structures, have been widely studied because of their beneficial properties and have been used in wastewater treatment and other applications such as bio-sensing, biomedical engineering, agriculture and horticulture, drug delivery, and sanitary products (11-14).

However, hydrogel made purely from synthetic materials and metal ions have their drawbacks due

to their environmental impact and toxicity to living cells when used as an antibacterial agent (15). Moreover, nanoparticle-based hydrogel development has been restricted due to their physical and chemical instability (16). To address these drawbacks, researchers have focused on synthesizing polysaccharide-based hydrogel, which can be prepared by polymer grafting and cross-linking reactions, making them more beneficial as adsorbents than conventional hydrogels. This is not only because of the hydrophilic groups, such as $-\text{OH}$, $-\text{NH}_2$, $-\text{COOH}$, and $-\text{CONH}_2$ on their surface that help in the adsorption of the pollutants via electrostatic interaction and hydrogen bonding, but due to their low-cost, non-toxic, environmentally friendly, and highly biodegradable and biocompatible nature (17-19, 3).

Chitosan is a deacetylated version of chitin (the second most abundant natural polysaccharide biopolymer after cellulose). It is made up of 2-acetamido-2-deoxy- β -D-glucopyranose and 2-amino-2-deoxy- β -D-glucopyranose linked by $\beta(1,4)$ -linkage and possesses important properties of biopolymers such as non-toxicity, biocompatibility, and biodegradability than chitin (20,21). In addition, chitosan has positive charges on its surface, which helps when bonding with negatively charged groups, thus making it a compelling candidate in wastewater remediation. Despite the advantages of using chitosan, there are disadvantages associated with its use, namely low porosity, low thermal resistance, high solubility, and low stability in acidic medium (20,21). These disadvantages limit its use, especially in the adsorption of acidic pollutants such as dyes from their aqueous solutions. Modifying the chitosan chains is crucial to avert these challenges and improve performance. Hence, techniques such as crosslinking, blending with other polymers, and grafting copolymerization have been used to achieve it (22-25).

Therefore, to prevent the aforementioned limitations of chitosan and to improve its ability to remove dyes from aqueous solutions, we synthesized a new adsorbent material (hydrogel) in this study by blending chitosan with trichlorovinylsilane and subsequent cross-linking with polyacrylamide. To the best of our knowledge, no previous work has reported using this material to remove dye (methylene blue) from an aqueous solution. The effect of different parameters such as adsorbent dosage, temperature, initial concentration of dye, contact time, and pH on the adsorption process was investigated to understand the adsorption process's kinetics and equilibrium adsorption isotherms.

2. MATERIALS AND METHODS

2.1. Materials

Low molecular weight (LMW) chitosan (75-85 % DDA) was purchased from Sigma-Aldrich Co. (St. Louis, USA) and used as supplied. Acetone and acetic acid were purchased from Merck, Germany. Trichlorovinylsilane, acrylamide, N,N'-Methylenebisacrylamide, Methylene blue (MB) and ammonium

persulfate were obtained from Sigma-Aldrich, Germany.

2.2. Synthesis of Trichlorovinylsilane Chitosan-g-acrylamide Hydrogel (VSi-CTS-g-PAAm)

4 g of low molecular weight chitosan (CTS) was weighed into a bottle; 10 mL of trichlorovinylsilane (VSi) was added and allowed to soak the chitosan for 3 days. After complete soaking and interaction with chitosan, the bottle was opened and excess fumes of trichlorovinylsilane allowed to escape. The product (VSi-CTS) produced was properly stored in a corked container.

50 mL of 2.5 % acetic acid was added into a conical flask containing 0.5 g of VSi-CTS, and it was allowed to stir overnight until complete dissolution. 10 mL of the VSi-CTS acetic acid solution was used in the preparation of the hydrogel by adding varying amount of acrylamide (0.9 g, 0.7 g, 0.5 g, 0.3 g), 0.05 g N,N'-methylenebisacrylamide (crosslinker) and 0.05 g ammonium persulfate (initiator). The reaction was carried out at 75 °C until gel was formed.

Finally, the synthesized hydrogel was washed several times with distilled water and acetone, and then dried at room temperature until a constant weight was obtained.

2.3. Adsorption Experiments

Batch adsorption experiments were performed at 25 – 50 °C temperature range using a set of 250 mL Erlenmeyer flask containing 0.025 g of adsorbent and 25 mL of MB solution of different initial concentrations (10 – 100 mg/L). The MB solution was adjusted to varying pH range (2 – 12) using 0.1 M HCl and 0.1 M NaOH solutions. It was then shaken at an agitation speed of 205 rpm for 24 h (1440 min). After equilibrium is achieved, decantation and filtration were carried out and the equilibrium concentration of the dye was determined using a UV-visible spectrophotometer (2377 double beam) at maximum wavelength of 665 nm. The percentage removal of MB dye and amount of dye adsorbed were calculated using the following equations.

$$\% \text{ Removal} = \frac{(C_0 - C_e)}{C_0} \times 100 \quad (1)$$

$$q_e = \frac{(C_0 - C_e)}{M} V \quad (2)$$

where C_0 and C_e (mg/L) are the initial dye concentration and equilibrium dye concentration at a given time, q_e (mg/g) amount of MB dye in mg per gram of adsorbent, V (dm^3) volume of solution, M (g) mass of hydrogel used.

3. RESULTS AND DISCUSSION

3.1. Effect of Adsorbent Dosage on the Adsorption Process

The effect of adsorbent dosage was studied using 0.025 – 0.075 g, 25 mL of 10 mg/L adsorbate at 25 °C, pH 12 for 24 h. As can be seen in Figure 1, the adsorption efficiency of the adsorbent was very high at low adsorbent dosage and remained almost stable

with increase the adsorbent dosage. The observed trend under the studied conditions could be attributed to the presence of large numbers of active adsorption sites on the adsorbent, which made it possible for the high adsorption efficiency to be

recorded at low adsorbent dosage. This study result is consistent with previous studies, which reported adsorption sites to be responsible for high adsorption efficiency of adsorbents (26,27).

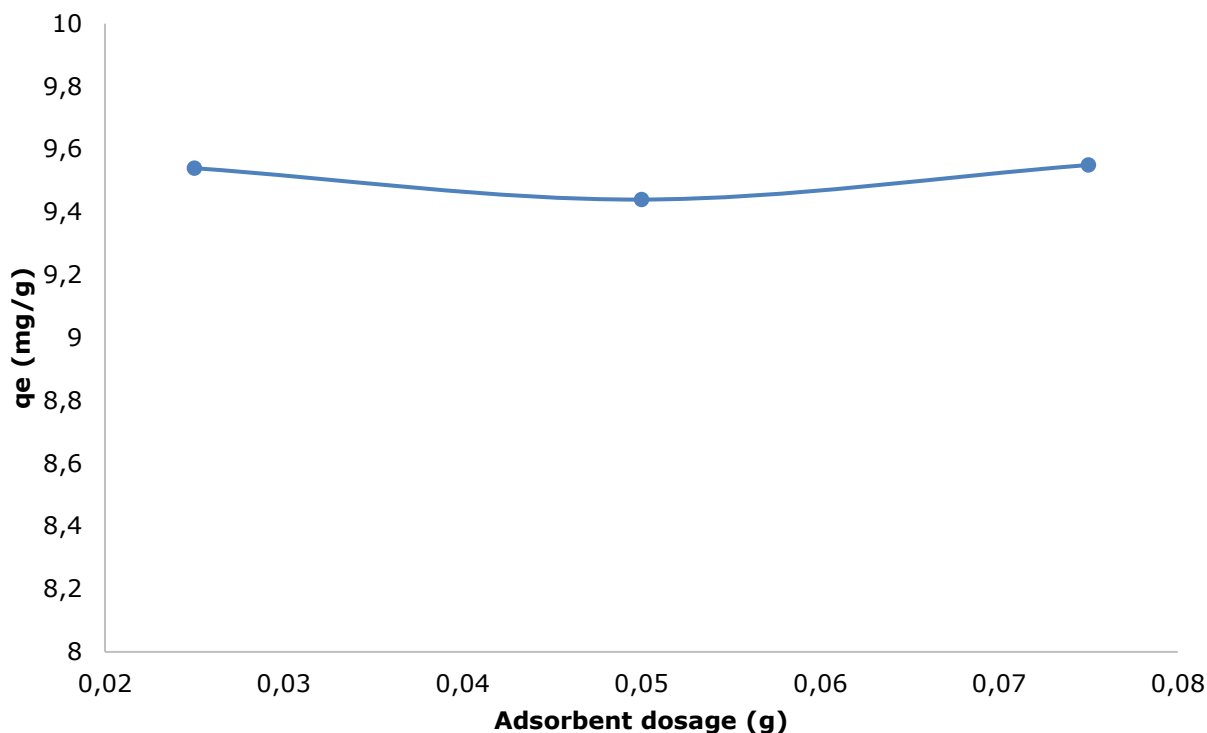


Figure 1: Effect of adsorbent dosage on the adsorption of MB onto VSi-CTS-g-PAAm hydrogel.

3.2. Effect of Initial Dye Concentration and Adsorption Isotherm

The effect of initial concentration on the amount of MB adsorbed is shown in Figure 2. Different concentrations of MB were prepared ranging from 10 – 120 mg/L and the experiment was carried out at 25 °C, pH 12, with 0.025 g of the adsorbent for 24 h. As the concentration of MB increases there was an increase in the uptake of MB dye onto VSi-CTS-g-PAAm hydrogel. This could be attributed to increased collisions between the dye molecules as a result of bulk density of the dye molecules thereby prevailing over any liquid to solid phase barrier (28,29). Nevertheless, as the adsorbent active sites continued to bind to the dye molecules, it got to a point of saturation (100 mg/L), and further increase in MB concentration led to decrease in the amount of dye molecules adsorbed.

To fully understand the adsorption behavior of the prepared VSi-CTS-g-PAAm hydrogel, the Langmuir and Freundlich adsorption isotherm models were used. The linearized forms of their equations are given in equations 3 and 4 respectively.

$$\frac{1}{q_e} = \frac{1}{q_m} + \frac{1}{K_L q_m C_e} \quad (3) \text{ Langmuir model}$$

$$\ln q_e = \ln K_F + \frac{1}{n} \ln C_e \quad (4) \text{ Freundlich model}$$

Where C_e is the (mg/dm³) is the equilibrium dye concentration in solution, q_e (mg/g) is the equi-

librium dye concentration on the adsorbent, q_m (mg/g) is the MB concentration onto the adsorbent when monolayer forms, C_0 (mg/dm³) is the initial dye concentration, and K_L is the Langmuir constant (dm³/mg).

Figures 3 and 4 illustrate the different isotherms of Langmuir and Freundlich respectively. The obtained experimental data fitted well into the two models. However, the correlation coefficient for Langmuir ($R^2 = 0.986$) was observed to be a better fit with a maximum adsorption capacity of 68.02 mg/g. The values for the parameters in the Langmuir and Freundlich are summarized in Table 1. The most important feature of the Langmuir isotherm is the R_L , which is known as the dimensionless constant separation factor that helps to foretell if an adsorption system is favorable or unfavorable and is given by equation (5). Adsorption system is favorable when ($0 < R_L < 1$), unfavorable ($R_L > 1$), linear ($R_L = 1$), irreversible ($R_L = 0$) (30,31).

$$R_L = \frac{1}{1 + K_L C_0} \quad (5) \text{ Separation factor}$$

The plot of the Separation Factor is shown in Figure 5. The R_L values obtained ranged from 0.283–0.703, indicating that the monolayer adsorption of MB onto VSi-CTS-g-PAAm hydrogel was favorable. It also established that the adsorption data fitted into the Langmuir isotherm at the optimal conditions in this study (30,31).

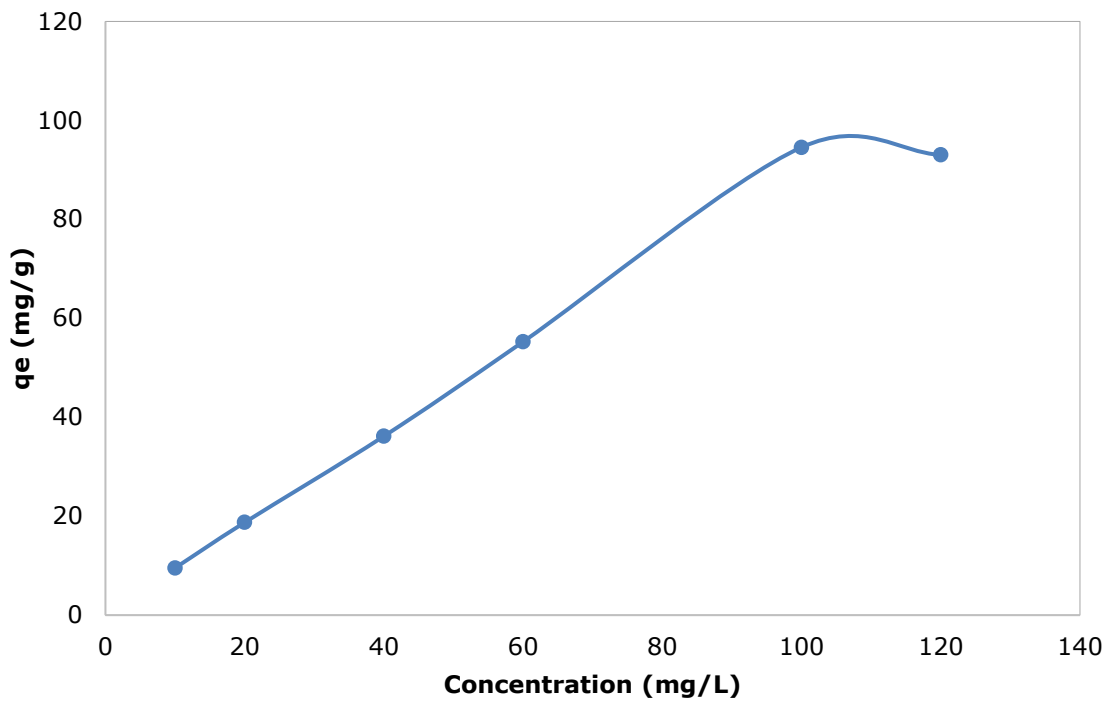


Figure 2: Effect of initial dye concentration on the adsorption of MB onto VSi-CTS-g-PAAm hydrogel.

Table 1: Summary of adsorption isotherm parameters.

q _m (mg/g)	Langmuir model			Freundlich model		
	K _L	R _L	R ²	n	K _F	R ²
68.02	0.042	0.283-0.703	0.986	1.42	1.21	0.978

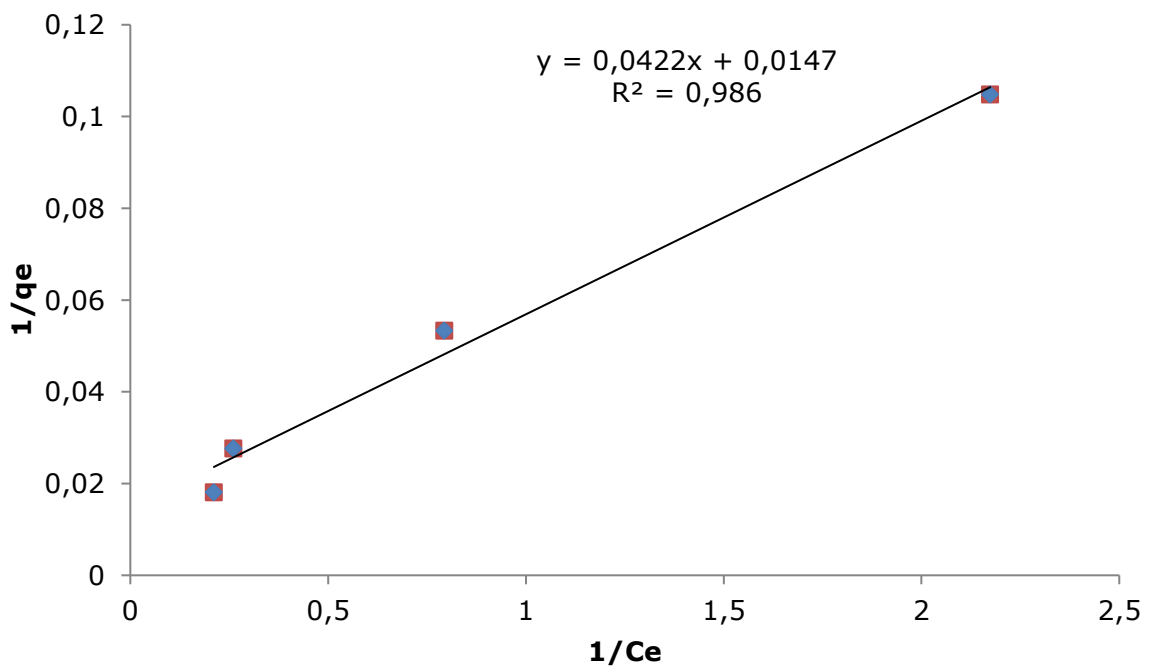


Figure 3: Langmuir adsorption Isotherm for the adsorption of MB onto VSi-CTS-g-PAAm hydrogel.

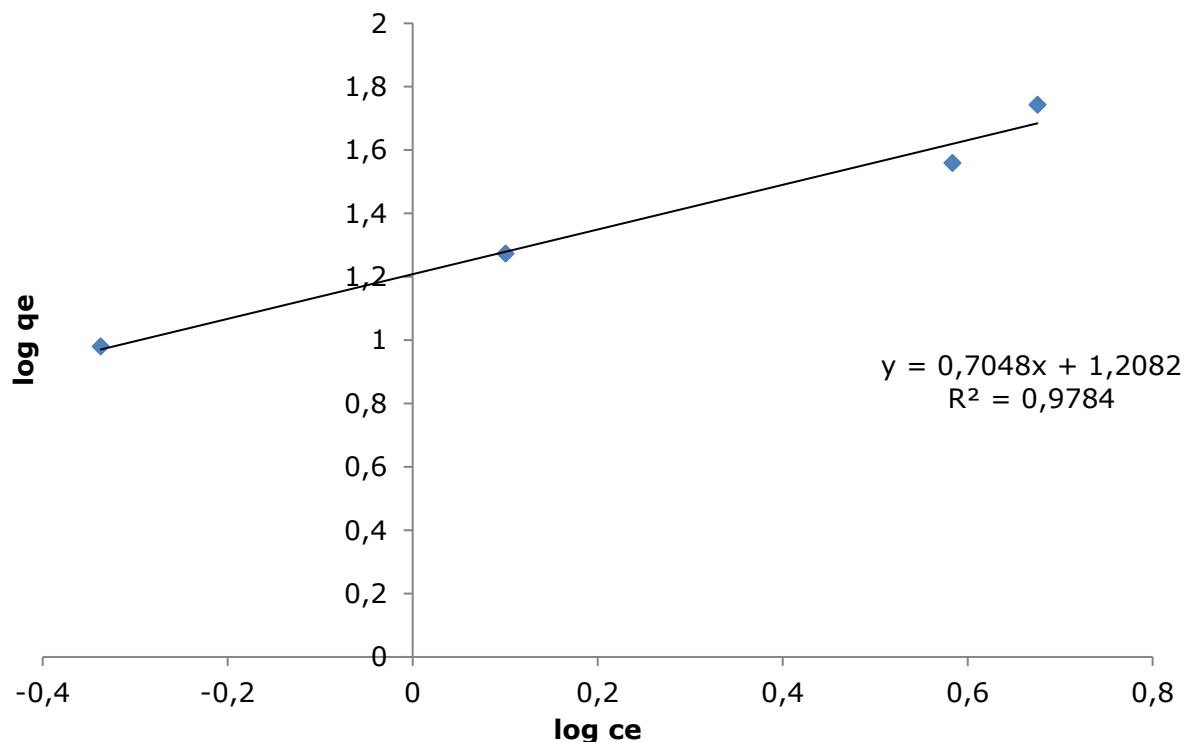


Figure 4: Freundlich adsorption isotherm for the adsorption of MB onto VSi-CTS-g-PAAm hydrogel.

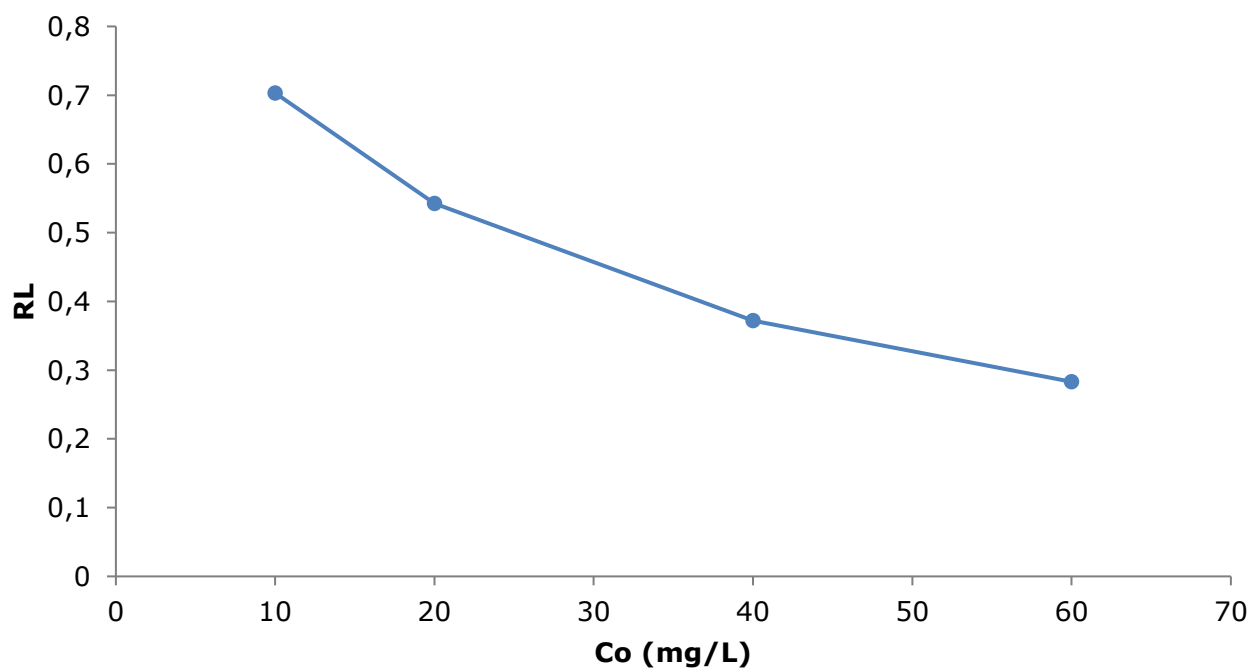


Figure 5: Separation factor R_L versus the initial MB dye concentration at 25 °C.

3.3. Effect of pH on The Adsorption Process

The effect of pH of the dye solution was studied using 0.025 g of the adsorbent, 25 mL of 10 mg/L adsorbate at 25 °C for 24 h, while the pH was varied between 2-12. From the results obtained the adsorption of MB increased with increase in the pH as can be seen from Fig. 6 with the maximum

adsorption occurring at pH 12. The observed trend is as a result of protonation of functional groups such as carboxyl and alcoholic groups at pH < 3 that decreased the adsorption efficiency, while deprotonation of these functional groups occurs at pH > 8 and increases the adsorption efficiency (32).

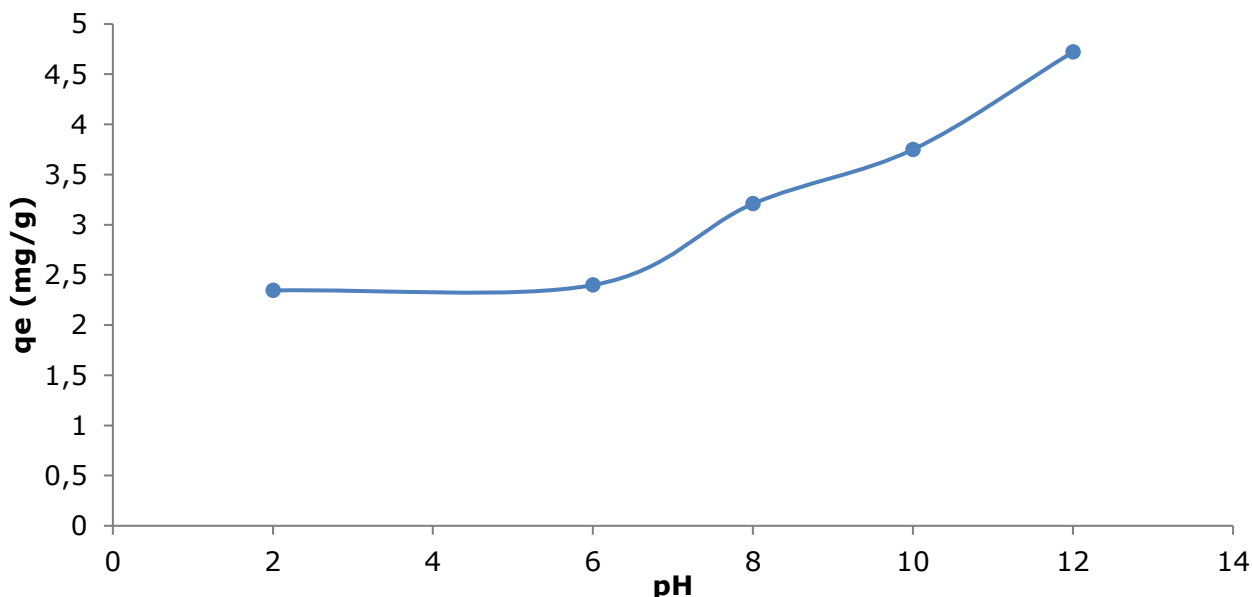


Figure 6: Effect of pH on the adsorption of MB onto VSi-CTS-g-PAAm hydrogel.

3.4. Effect of Temperature on the Adsorption Process

The effect of temperature on the adsorption of MB onto VSi-CTS-g-PAAm was performed at 25, 35 and 50 °C for 24 h using 25 mL of 10 mg/L adsorbate solution and 0.025 g of adsorbate at pH 12. There was an increase in the adsorption of MB as the temperature was increased signifying an endother-

mic process (27). The adsorption capacity of MB increased from 4.722 – 9.777 mg/g onto the VSi-CTS-g-PAAm hydrogel at 25 – 50 °C as seen from Fig. 7. This can be ascribed to the increase in the kinetic energy of the MB molecules giving them adequate energy to prevail over the bulk layer and be adsorbed onto the crevice of the hydrogel network (33).

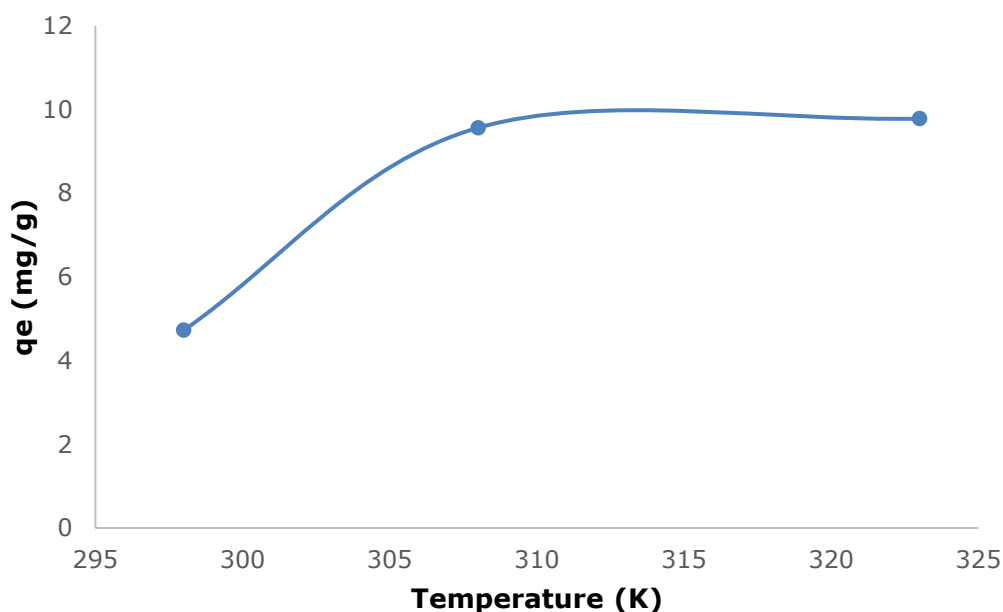


Figure 7: Effect of temperature on the adsorption of MB onto VSi-CTS-g-PAAm hydrogel.

3.5. Effect of Time and Adsorption Kinetics

The effect of contact time of the adsorbent with MB was studied from 30 – 1440 min (0.5 – 24 h) using an adsorbent dosage of 0.025 g, 25 mL of 10 mg/L adsorbate at pH 12. The result obtained is as presented in Fig. 8. It can be seen that the quantity of MB adsorbed increased rapidly at the beginning and became gradual afterward until equilibrium was

achieved. The optimum time was attained at 1440 min; thereafter, the percentage of dye adsorption remained relatively constant. The increase in adsorption ab initio could be attributed to many vacant adsorption sites; these sites became occupied over time, resulting in reduced adsorption of MB (28). A similar trend in adsorption has been previously reported (27).

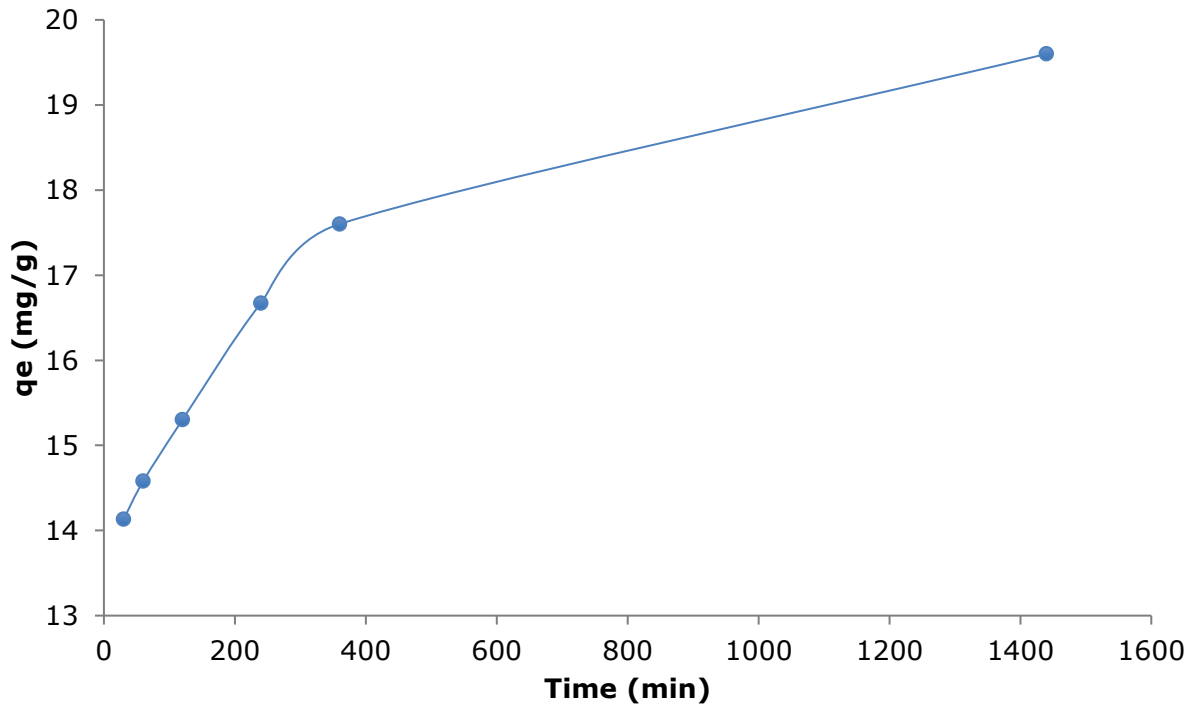


Figure 8: Effect of time on the adsorption of MB onto VSi-CTS-g-PAAm hydrogel.

Two kinetic models, namely the pseudo-first order and pseudo-second orders (Equations 6 and 7, respectively), were used to fit the experimental data and propose a mechanism for the adsorption process. The results are presented in Fig. 9 and 10, respectively. The correlation coefficient (R^2) values obtained show that the experimental data better fits into the pseudo-second-order kinetic model. This suggests that a pseudo-second-order kinetic model could be applied in describing the entire adsorption

process, with chemisorption as the rate-determining step (27). The kinetics parameters for the adsorption of MB onto VSi-CTS-g-PAAm hydrogel are presented in Table 2.

$$\ln(q_e - q_t) = \ln(q_e) - (K_1)t \quad (6) \text{ Pseudo first order}$$

$$\frac{t}{q_t} = \frac{1}{k_2 q_e^2} + \frac{t}{q_e} \quad (7) \text{ Pseudo second order}$$

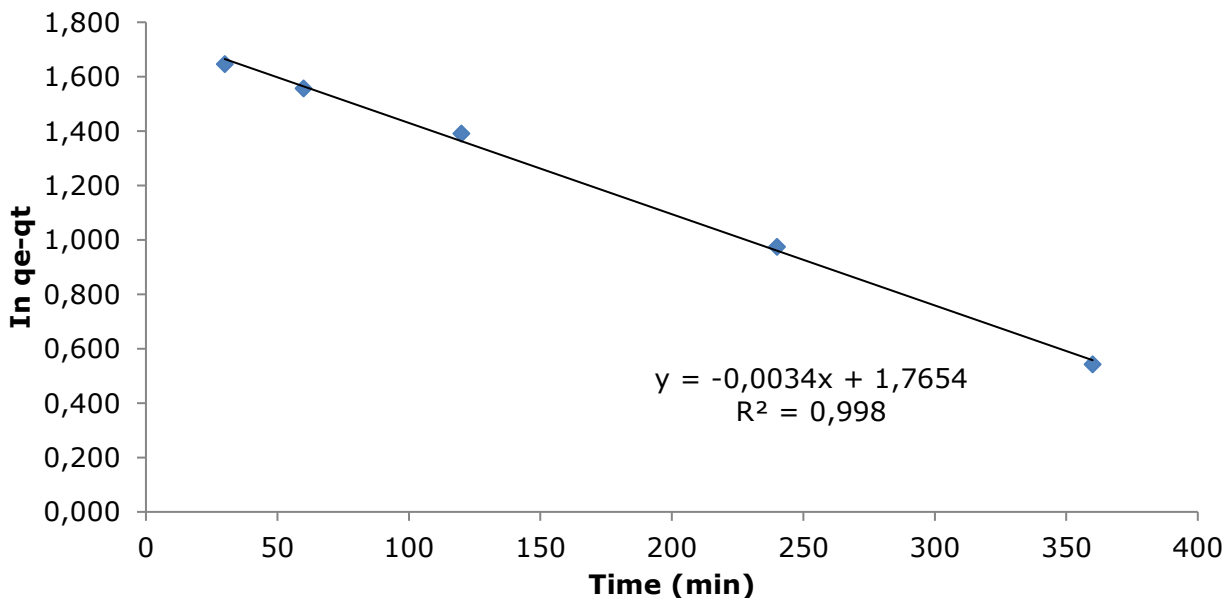


Figure 9: Pseudo-first-order kinetics for the adsorption of MB onto VSi-CTS-g-PAAm hydrogel.

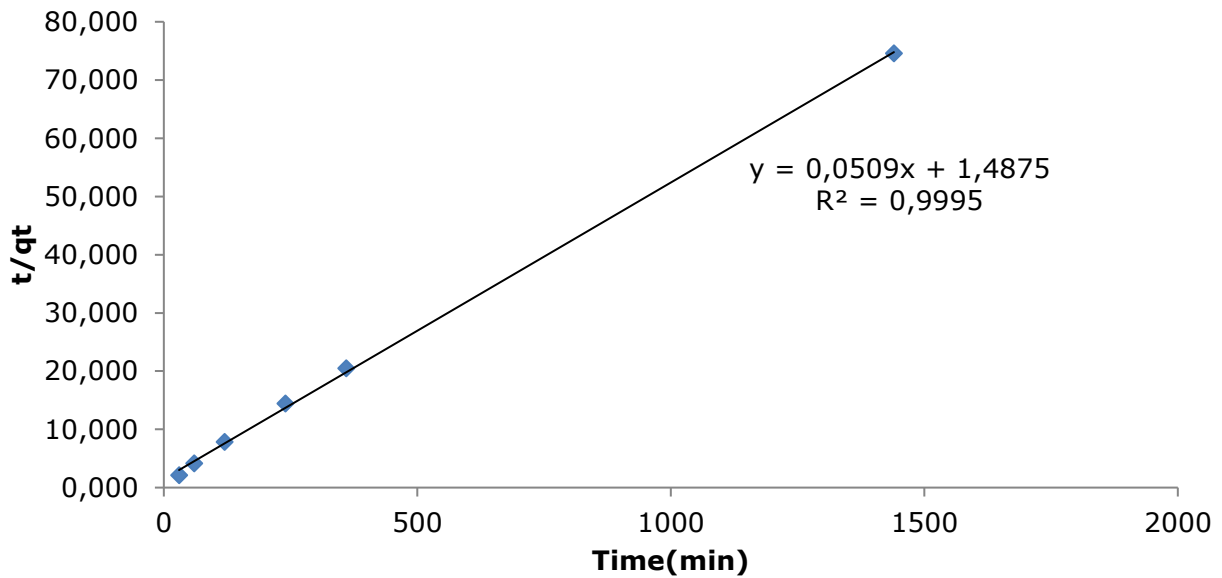


Figure 10: Pseudo-second-order kinetics for the adsorption of MB onto VSi-CTS-g-PAAm hydrogel.

Table 2: Kinetic parameters for the adsorption of MB onto VSi-CTS-g-PAAm hydrogel

Kinetic Model	Parameter	Value
Pseudo first order model	K_1 (min^{-1})	0.0034
	R^2	0.998
Pseudo second order model	K_2 ($\text{gmg}^{-1}\text{min}^{-1}$)	1.4875
	R^2	0.999
Boyd model	R^2	0.998

To get further information regarding the mechanism of the adsorption process, the experimental data was fitted into the Boyd kinetic model using equation 8, and the result is shown in Figure 11. It can be seen that the straight does not pass through the origin; therefore, film diffusion or bulk mass transport mechanism could be suggested for the sorption

process, which may be attributed to electrostatic interaction between the VSi-CTS-g-PAAm hydrogel surface and the cationic MB dye molecules (34).

$$B_t = -0.4978 - \ln\left(1 - \frac{qt}{q\alpha}\right) \quad (8) \text{ Boyd kinetic model}$$

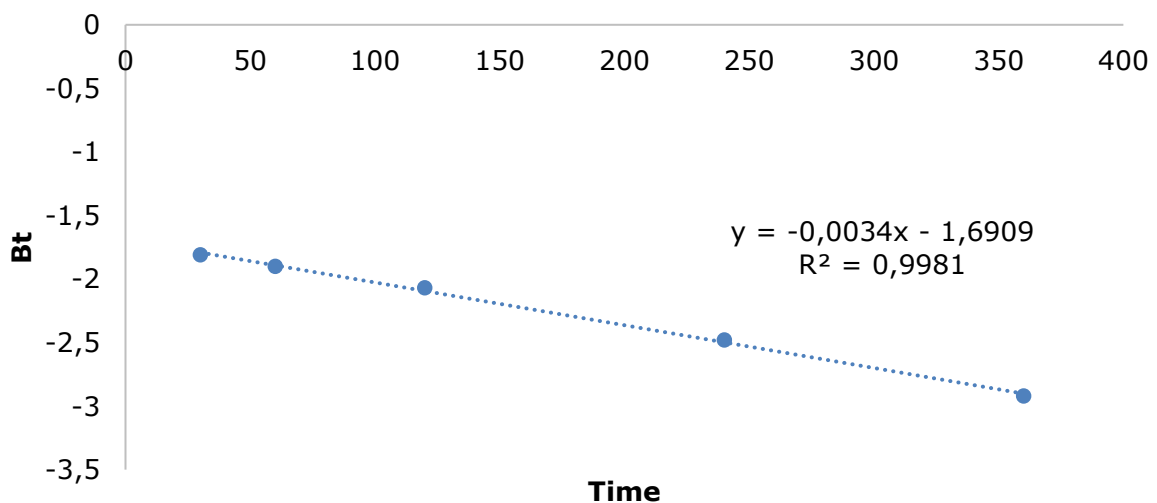


Figure 11: Boyd kinetic model for MB adsorption onto VSi-CTS-PAAm.

4. CONCLUSION

Hydrogels prepared as VSi-CTS-g-PAAm were tested for the adsorption of MB dye from an aqueous solution. The study's findings indicate that several

elements, including the adsorbent dosage, the adsorbate concentration, the duration of contact, the pH level, and the temperature, influence the adsorption process. The obtained experimental data exhibited a favorable agreement with the Langmuir

isotherm model, indicating that the adsorption process adhered to a chemisorption mechanism, as evidenced by the pseudo-second-order kinetic behavior. The adsorption process was hypothesized to occur by either film diffusion or bulk mass transfer mechanisms, as indicated by the plot of the Boyd kinetic model. The hydrogel, known as VSi-CTS-g-PAAm, has been successfully synthesized and demonstrates the ability to adsorb methylene blue (MB) from aqueous solutions. This characteristic makes it a promising candidate for potential utilization in the remediation of wastewater contaminated with dyes.

5. CONFLICT OF INTEREST

There is no conflict of interest to declare.

6. REFERENCES

- Ogugbue CJ, Sawidis T. Bioremediation and detoxification of synthetic wastewater containing triarylmethane dyes by *Aeromonas hydrophila* Isolated from Industrial Effluent. *Biotechnol Res Int* [Internet]. 2011 Jul 25;2011:967925. Available from: [<URL>](#).
- Samchetshabam G, Hussan A, Choudhury TG. Impact of textile dyes waste on aquatic environments and its treatment revival of fisheries cooperatives and fisheries federation of Assam View project Hilsa Project View project. *Environ Ecol* [Internet]. 2017;35(3C):2349–53. Available from: [<URL>](#).
- Cai J, Zhang D, Xu W, Ding W-P, Zhu Z-Z, He J-R, et al. Polysaccharide-based hydrogels derived from cellulose: the architecture change from nanofibers to hydrogels for a putative dual function in dye wastewater treatment. *J Agric Food Chem* [Internet]. 2020 Sep 9;68(36):9725–32. Available from: [<URL>](#).
- Hameed BH. Spent tea leaves: A new non-conventional and low-cost adsorbent for removal of basic dye from aqueous solutions. *J Hazard Mater* [Internet]. 2009 Jan 30;161(2–3):753–9. Available from: [<URL>](#).
- Salleh MAM, Mahmoud DK, Karim WAWA, Idris A. Cationic and anionic dye adsorption by agricultural solid wastes: A comprehensive review. *Desalination* [Internet]. 2011 Oct 3;280(1–3):1–13. Available from: [<URL>](#).
- Bhatti HN, Akhtar N, Saleem N. Adsorptive Removal of Methylene Blue by Low-Cost Citrus sinensis Bagasse: Equilibrium, Kinetic and Thermodynamic Characterization. *Arab J Sci Eng* [Internet]. 2012 Jan 13;37(1):9–18. Available from: [<URL>](#).
- Bhatti HN, Safa Y. Removal of anionic dyes by rice milling waste from synthetic effluents: equilibrium and thermodynamic studies. *Desalin Water Treat* [Internet]. 2012 Oct;48(1–3):267–77. Available from: [<URL>](#).
- Mittal A, Jain R, Mittal J, Varshney S, Sikarwar S. Removal of Yellow ME 7 GL from industrial effluent using electrochemical and adsorption techniques. *Int J Environ Pollut* [Internet]. 2010;43(4):308–23. Available from: [<URL>](#).
- Daraei H, Mittal A, Noorisepehr M, Mittal J. Separation of chromium from water samples using eggshell powder as a low-cost sorbent: kinetic and thermodynamic studies. *Desalin Water Treat* [Internet]. 2015 Jan 2;53(1):214–20. Available from: [<URL>](#).
- Noreen S, Bhatti HN, Nausheen S, Sadaf S, Ashfaq M. Batch and fixed bed adsorption study for the removal of Drimarine Black CL-B dye from aqueous solution using a lignocellulosic waste: A cost affective adsorbent. *Ind Crops Prod* [Internet]. 2013 Oct 1;50:568–79. Available from: [<URL>](#).
- Puoci F, Iemma F, Spizzirri UG, Cirillo G, Curcio M, Picci N. Polymer in Agriculture: a Review. *Am J Agric Biol Sci* [Internet]. 2008 Jan 1;3(1):299–314. Available from: [<URL>](#).
- Kosemund K, Schlatter H, Ochsenhirt JL, Krause EL, Marsman DS, Erasala GN. Safety evaluation of superabsorbent baby diapers. *Regul Toxicol Pharmacol* [Internet]. 2009 Mar 1;53(2):81–9. Available from: [<URL>](#).
- Buenger D, Topuz F, Groll J. Hydrogels in sensing applications. *Prog Polym Sci* [Internet]. 2012 Dec 1;37(12):1678–719. Available from: [<URL>](#).
- Holback H, Yeo Y, Park K. Hydrogel swelling behavior and its biomedical applications. In: *Biomedical Hydrogels* [Internet]. Elsevier; 2011. p. 3–24. Available from: [<URL>](#).
- Grade S, Eberhard J, Neumeister A, Wagener P, Winkel A, Stiesch M, et al. Serum albumin reduces the antibacterial and cytotoxic effects of hydrogel-embedded colloidal silver nanoparticles. *RSC Adv* [Internet]. 2012 Jul 30;2(18):7190. Available from: [<URL>](#).
- Li S, Dong S, Xu W, Tu S, Yan L, Zhao C, et al. Antibacterial Hydrogels. *Adv Sci* [Internet]. 2018 May 1;5(5):1700527. Available from: [<URL>](#).
- Yang J, Chen Y, Zhao L, Feng Z, Peng K, Wei A, et al. Preparation of a chitosan/carboxymethyl chitosan/AgNPs polyelectrolyte composite physical hydrogel with self-healing ability, antibacterial properties, and good biosafety simultaneously, and its application as a wound dressing. *Compos Part B Eng* [Internet]. 2020 Sep 15;197:108139. Available from: [<URL>](#).
- Lu H, Wang X, Shi X, Yu K, Fu YQ. A phenomenological model for dynamic response of double-network hydrogel composite undergoing transient transition. *Compos Part B Eng* [Internet]. 2018 Oct 15;151:148–53. Available from: [<URL>](#).
- Jana S, Pradhan SS, Tripathy T. Poly(N,N-dimethylacrylamide-co-acrylamide) Grafted hydroxyethyl cellulose hydrogel: a useful congo red dye remover. *J Polym Environ* [Internet]. 2018 Jul

- 13;26(7):2730–47. Available from: [<URL>](#).
20. Ravi Kumar MN. A review of chitin and chitosan applications. *React Funct Polym* [Internet]. 2000 Nov 1;46(1):1–27. Available from: [<URL>](#).
21. Al-Harby NF, Albahly EF, Mohamed NA. Synthesis and characterization of novel uracil-modified chitosan as a promising adsorbent for efficient removal of congo red dye. *Polymers (Basel)* [Internet]. 2022 Jan 10;14(2):271. Available from: [<URL>](#).
22. Mohamed NA, Abd El-Ghany NA. Synthesis, characterization, and antimicrobial activity of carboxymethyl chitosan-graft-poly(n-acryloyl, n'-cyanoacetohydrazide) copolymers. *J Carbohydr Chem* [Internet]. 2012 Mar 1;31(3):220–40. Available from: [<URL>](#).
23. Abraham A, Solomon PA, Rejini VO. Preparation of chitosan-polyvinyl alcohol blends and studies on thermal and mechanical properties. *Procedia Technol* [Internet]. 2016 Jan 1;24:741–8. Available from: [<URL>](#).
24. Elmehbad NY, Mohamed NA. Terephthalohydrazido cross-linked chitosan hydrogels: synthesis, characterization and applications. *Int J Polym Mater Polym Biomater* [Internet]. 2022 Sep 2;71(13):969–82. Available from: [<URL>](#).
25. Elsayed NH, Monier M, Youssef I. Fabrication of photo-active trans -3-(4-pyridyl)acrylic acid modified chitosan. *Carbohydr Polym* [Internet]. 2017 Sep 15;172:1–10. Available from: [<URL>](#).
26. Anwar J, Shafique U, Waheed-uz-Zaman, Salman M, Dar A, Anwar S. Removal of Pb(II) and Cd(II) from water by adsorption on peels of banana. *Bioresour Technol* [Internet]. 2010 Mar 1;101(6):1752–5. Available from: [<URL>](#).
27. Elaigwu SE, Rocher V, Kyriakou G, Greenway GM. Removal of Pb²⁺ and Cd²⁺ from aqueous solution using chars from pyrolysis and microwave-assisted hydrothermal carbonization of *Prosopis africana* shell. *J Ind Eng Chem* [Internet]. 2014 Sep 25;20(5):3467–73. Available from: [<URL>](#).
28. Olgun A, Atar N. Equilibrium, thermodynamic and kinetic studies for the adsorption of lead (II) and nickel (II) onto clay mixture containing boron impurity. *J Ind Eng Chem* [Internet]. 2012 Sep 25;18(5):1751–7. Available from: [<URL>](#).
29. Shokry A, El Tahan A, Ibrahim H, Soliman M, Ebrahim S. Polyaniline/akaganeite superparamagnetic nanocomposite for cadmium uptake from polluted water. *Desalin Water Treat* [Internet]. 2019;171:205–15. Available from: [<URL>](#).
30. Bamgbose JT, Elaigwu SE, Adimula VO, Okeowo HO, Olayemi VT, Ameen OA, et al. Green route synthesis and adsorption studies of copper-benzimidazole coordination polymer for removal of methyl orange from water. *Chem Africa* [Internet]. 2023 Apr 14;Article in Press:1–12. Available from: [<URL>](#).
31. Tella AC, Bamgbose JT, Adimula VO, Omotoso M, Elaigwu SE, Olayemi VT, et al. Synthesis of metal-organic frameworks (MOFs) MIL-100(Fe) functionalized with thioglycolic acid and ethylenediamine for removal of eosin B dye from aqueous solution. *SN Appl Sci* [Internet]. 2021 Jan 13;3(1):136. Available from: [<URL>](#).
32. Al-qudah YHF, Mahmoud GA, Abdel Khalek MA. Radiation crosslinked poly (vinyl alcohol)/acrylic acid copolymer for removal of heavy metal ions from aqueous solutions. *J Radiat Res Appl Sci* [Internet]. 2014 Apr 1;7(2):135–45. Available from: [<URL>](#).
33. Chen X, Chen G, Chen L, Chen Y, Lehmann J, McBride MB, et al. Adsorption of copper and zinc by biochars produced from pyrolysis of hardwood and corn straw in aqueous solution. *Bioresour Technol* [Internet]. 2011 Oct 1;102(19):8877–84. Available from: [<URL>](#).
34. Elkady MF, El-Aassar MR, Hassan HS. Adsorption profile of basic dye onto novel fabricated carboxylated functionalized co-polymer nanofibers. *Polymers (Basel)* [Internet]. 2016 Apr 29 [cited 2023 Sep 5];8(5):177. Available from: [<URL>](#).